Pseudomagnetic Fields and Ballistic Transport in a Suspended Graphene Sheet

M. M. Fogler,[1] F. Guinea,[2] and M. I. Katsnelson[3]

[1]*Department of Physics, University of California San Diego, 9500 Gilman Dr., La Jolla, California 92093, USA*
[2]*Instituto de Ciencia de Materiales de Madrid (CSIC), Sor Juana Inés de la Cruz 3, Madrid 28049, Spain, and Donostia International Physics Center (DIPC), Paseo Manuel de Lendizábal 4, San Sebastián, E-20018, Spain*
[3]*Institute for Molecules and Materials, Radboud University Nijmegen, Heijendaalseweg 135, 6525 AJ, Nijmegen, The Netherlands*

(Received 20 July 2008; published 25 November 2008)

We study a suspended graphene sheet subject to the electric field of a gate underneath. We compute the elastic deformation of the sheet and the corresponding effective gauge field, which modifies the electronic transport. In a clean system the two-terminal conductance of the sample is reduced below the ballistic limit and is almost totally suppressed at low carrier concentrations in samples under tension. Residual disorder restores a small finite conductivity.

DOI: 10.1103/PhysRevLett.101.226804 PACS numbers: 73.23.Ad, 72.10.Fk, 73.50.−h

Introduction and results.—Graphene layers which are one or a few carbon atoms thick [1,2] combine a novel electronic spectrum (''massless Dirac fermions'' [2,3]) and unusual structural and mechanical properties [4–9]. (For general reviews, see Refs. [10–12].) Originally, graphene sheets lying on a quartz substrate were prepared and investigated but later it turned out that the freely hanged membranes of macroscopically large sizes can be derived [4]. The electronic and mechanical properties of these membranes are being intensively studied [5–9,13–16]. They demonstrate a much higher electron mobility than graphene sheets on a substrate [13,14,16] and extraordinary mechanical stiffness [7,8], which makes them especially interesting for applications.

Below we show that unavoidable deformations of the membranes by an applied electric field can strongly affect their transport properties. As a model, we consider a strip of graphene clamped at two parallel edges $x = \pm L/2$, see Fig. 1(a). The strip is suspended above a control gate, whose electric field induces electron concentration n in graphene and exerts on it the pressure $P = (2\pi e^2 n^2)/\epsilon$. We assume that the length of the strip in the undeformed state is $L + \Delta L$, where the ''slack'' ΔL can be of either sign. Negative ΔL implies the sheet is under tension already at $P = 0$.

Our main results include the deformation h_0 and the ballistic conductance G as a function of n. They are shown in Figs. 2(a) and 3, respectively, for three representative ΔL. We also derive the analytical formula

$$G(n) \simeq \frac{e^2}{h}\left(\frac{4}{\pi}k_F - |A_y|\right)W, \tag{1}$$

where W is the width of the sample, $k_F = \sqrt{\pi|n|}$ is the Fermi wave vector, and A_y of dimension of inverse length is related to the deformation [Fig. 2(b) and Eq. (6)]. Equation (1) is valid for $k_F \gg |A_y|$. In the opposite limit, which is realized for $\Delta L < 0$ (graphene initially under tension [7,9]) and small n, we find a nearly complete suppression of ballistic transport. The physical mechanism of this phenomenon is as follows. The deformation shifts the Dirac points by the amount A_y [Fig. 1(b)], which creates a mismatch between the graphene leads and the suspended region. If this shift exceeds the diameter $2k_F$ of the Fermi circle, the carriers are fully reflected.

Recent experiments [16] are in a qualitative agreement with Fig. 3(a); however, at very low n the conductivity tends to a *finite* value $\sim e^2/h$. We attribute this to disorder-assisted tunneling. Finally, we predict that if large n can be studied in future experiments, then G should become nonmonotonic with a maximum at

$$n = 3.1 \times 10^{12}\ \mathrm{cm}^{-2} \times (1\ \mu\mathrm{m}/L)^{4/5}, \tag{2}$$

which is roughly independent of ΔL, see Fig. 3(b).

Height profile.—Determining the profile $h(x)$ of a clamped elastic strip under a uniform load P is a standard problem of the elasticity theory. Under the condition

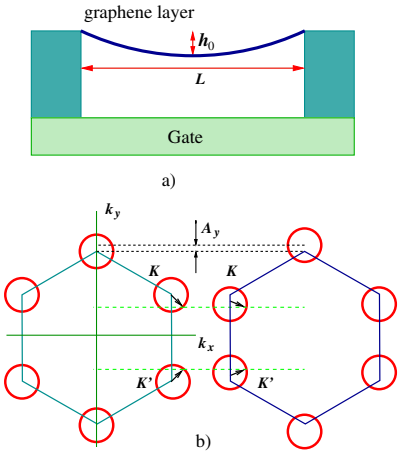

FIG. 1 (color online). (a) Sketch of the model of a suspended graphene sheet under consideration. (b) Fermi circle positions in the Brillouin zone in the leads (left) and in the suspended region (right).

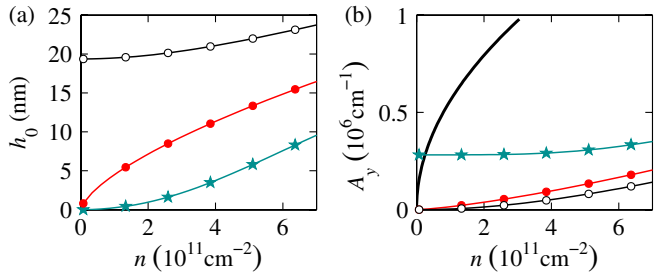

FIG. 2 (color online). (a) Deformation of a suspended graphene sheet of length $L = 1$ μm vs carrier concentration for three different ΔL (slack): -2 nm (stars), 0 nm (dots), and 2 nm (open circles). (b) The corresponding gauge potential. The top curve gives the Fermi wave vector $k_F(n)$.

$h_0 \equiv \max h(x) \ll L$ it has a well known analytic solution [17]. We focus on the case where n is either comparable or much larger than $n_0 = \sqrt{(16/\pi)(\epsilon\kappa)/(e^2L^3)} \approx (6 \times 10^9\ \mathrm{cm}^{-2})/(L/1\ \mu\mathrm{m})^{3/2}$, where $\kappa \approx 1.1$ eV is the bending rigidity of graphene [18]. In this case the deformation is nearly parabolic:

$$h(x) \simeq h_0\left(1 - \frac{4x^2}{L^2}\right), \qquad \frac{L}{2} - |x| \gg L\frac{\ln u}{u}, \tag{3}$$

where $u = (n/n_0)(L/h_0)^{1/2} \gg 1$. The maximum deformation h_0 is the positive root of the cubic equation

$$\left(h_0^2 - \frac{3}{16}L\Delta L\right)h_0 = \frac{3\pi}{64}\frac{e^2}{\epsilon E}(nL^2)^2, \tag{4}$$

where $E \approx 22$ eV/Å^2 is the two-dimensional Young's modulus of graphene [7,8]. At very large concentrations n, the height h_0 is given by the asymptotic formula

$$h_0 \simeq \left(\frac{3\pi}{64}\frac{e^2}{\epsilon E}n^2L^4\right)^{1/3}. \tag{5}$$

If n is not large, it is just as easy to solve Eq. (4) numerically. Representative results are plotted in Fig. 2(a).

The deformation induces perturbations of two types acting on electrons: the scalar potential $V(x)$ and the effective vector potential [19,20] $\mathbf{A}(x)$. We examine them below, starting with $\mathbf{A}(x)$.

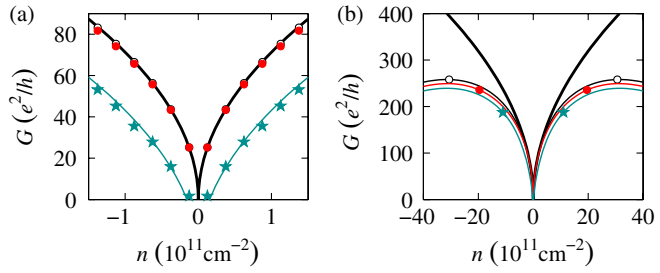

FIG. 3 (color online). Ballistic conductance for a sheet of width $W = 1$ μm over (a) narrow and (b) wide interval of n. ΔL and the symbols are the same as in Fig. 2. The thick curve is for the undeformed sheet. The thin lines represent Eq. (1).

Vector potential.—The shift of the Dirac points [Fig. 1(b)] is equivalent to the effect of a constant vector potential $\mathbf{A} = (A_x, A_y)$. We use this latter formalism in the following as it can be easily generalized to more complex situations. The role of $\mathbf{A}$ is the largest when the "zigzag" direction is along the y axis. Assuming this is the case, we obtain

$$A_x(x) = 0, \qquad A_y(x) = C_1\xi\frac{\beta}{a}\frac{t}{E} = C_1\xi\frac{\beta}{a}\frac{PL^2}{8Eh_0}, \tag{6}$$

where $\beta = -d\log(\gamma_0)/d\log(a) \approx 2$ is the dimensionless electron-phonon coupling parameter, $\gamma_0 \approx 3$ eV is the nearest neighbor hopping, $a \approx 1.4$ Å is the distance between nearest carbon atoms, $\xi = \pm 1$ is the valley index, $t \simeq PL^2/(8h_0)$ is the horizontal component of tension per unit length at the edges, and parameter $C_1 \sim 1$ is determined by the microscopic force constants [21,22]. The corresponding pseudomagnetic field $B(x) = -\partial_x A_y$ consists of two spikes at the edges $x = \pm L/2$.

Transport.—To compute the conductance G we assume perfect semi-infinite graphene leads of the same chemical potential at both ends of the strip. (In a more realistic situation the results should be corrected for the contact resistance in series with $1/G$.) Since the perturbations depend only on x, the k_y momentum is conserved. However, the pseudomagnetic field at the edges shifts the mechanical momentum, $k_y \to k_y - A_y$, of electrons inside the strip. This leads to partial reflection and, respectively, partial confinement for the quasiparticles approaching the edges from the outside and the inside of the strip. Similar effects have been previously examined in the context of Dirac particles subject to a nonuniform real magnetic field [23].

For $A_y = \mathrm{const}$, transmission coefficient $T(k_y)$ is

$$T(k_y) = \frac{k(0)^2k(A_y)^2}{k(0)^2k(A_y)^2 + k_F^2A_y^2\sin^2[k(A_y)L]}, \tag{7}$$

where $k(q) = \sqrt{k_F^2 - (k_y - q)^2}$. If $k(A_y)^2 < 0$, then $k(A_y)$ is pure imaginary, so that $\sin^2[k(A_y)L] \to -\sinh^2|k(A_y)L|$. In this case $T(k_y)$ is exponentially small. The plot of $T(k_y)$ is shown in the right-hand panel of Fig. 4 using the parametrization $k_y = k_F\sin\theta$ for $-\pi/2 < \theta < \pi/2$ and $n = 2 \times 10^{11}$ cm^{-2}. The transmission is indeed almost zero for a range of incident angles θ. In addition, Fabry-Pérot resonances appear because of the multiple scattering off the two interfaces.

Neglecting the contribution of edge channels, which is permissible when they are localized by disorder or the number of bulk channels k_FW/π is large, the conductance can be computed from

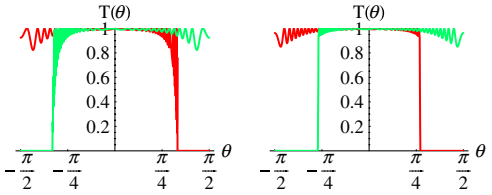

FIG. 4 (color online). Left-hand panel: Angular dependence of the transmission for $n = 2 \times 10^{11}$ cm^{-2}, no slack, and $L = 1$ μm. The two curves correspond to the two inequivalent Dirac points. Right-hand panel: Angular dependence of the transmission, including the effect of the scalar potential, Eq. (12).

$$G = \frac{4e^2}{h} W \int_{-k_F}^{k_F} \frac{dk_y}{2\pi} T(k_y). \tag{8}$$

In the case $k_F \gg |A_y|$ and $Lk_F \gg 1$ this integral reduces to a simple analytical formula (1) plotted in Fig. 3(b). As one can see, the deviations from the ballistic limit grow with n, making $G(n)$ nonmonotonic. The position of its maximum can be found from Eqs. (1), (5), and (6), which yield Eq. (2).

The behavior of G at small n crucially depends on the sign of ΔL. For $\Delta L \geq 0$, the effect of the gauge field becomes negligible. In contrast, for $\Delta L < 0$, the conductance becomes greatly suppressed. Thus, for $\Delta L = -2$ nm, it nearly vanishes at $|n| < 2.0 \times 10^{10}$ cm^{-2}, see Fig. 3(a).

Disorder effects.—Any real system contains disorder and its effect on conductance should be examined. We consider the experimentally relevant case [16] where (a) $\Delta L < 0$ and (b) the elastic mean-free path l is comparable to the system size L. In this situation disorder is important primarily at low n where it relaxes the constraint of momentum conservation, compensating for the momentum shift due to the gauge field.

For simplicity, we assume $1 \ll G/(4e^2/h) \ll k_F W$. In this regime the disorder is weak enough that its effect on the average conductance is still negligible yet it is strong enough to fully mix the transverse modes in the suspended region. The conductance is limited by the two interfaces $x = \pm L/2$, which act as classical resistors in series [24], $G = G_i/2$. Let us compute the conductance of a single interface G_i.

If disorder *near the interface* is neglected, G_i is given by the expression similar to Eq. (8) where $T(k_y)$ is now the transmission coefficient through a single interface: $T(k_y) = [4k(0)k(A)]/[\{k(0) + k(A)\}^2 + A_y^2]$. This formula holds if k_y mode is propagating, $\Im m k(0) = \Im m k(A_y) = 0$. Otherwise, it is evanescent and $T(k_y) = 0$. Each evanescent mode decays exponentially either to the left or to the right of $x = 0$ interface, depending on which of $\Im m k(0)$ and $\Im m k(A_y)$ is nonzero. At $k_F < |A_y|/2$ all modes at the Fermi energy are evanescent. Therefore, if the disorder is neglected, G_i vanishes.

Let us now include disorder-induced mixing among the evanescent and propagating modes, which gives a correction $\Delta T(k_y)$ to each $T(k_y)$. To the lowest order in the concentration n_s of scatterers, we find

$$\Delta T(k_y) = \int_{A_y - k_F}^{A_y + k_F} \frac{dk_y'}{2\pi} \int_{-\infty}^{\infty} dx n_s \delta T(k_y, k_y', x), \tag{9}$$

where $\delta T(k_y, k_y', x)$ is the off-diagonal transmission coefficient due to a single scatterer at $\mathbf{r} = (x, y)$. Function $\Delta T(k_y)$ has the dimension of length, similar to the transport cross section $\Lambda_s = 1/(n_s l)$. We expect $\delta T(k_y, k_y', x) \sim (\Lambda_s/k_F) \exp(-2|k(A_y)x|)$. Here the exponential represents the probability of the evanescent wave to reach the scatterer and the prefactor provides the correct units and scaling with disorder strength. The dominant contribution to $\Delta T(k_y)$ comes from the scatterers located in the strip $|x| \lesssim 1/|k(A_y)|$. Integrating over x, k_y, and k_y', we finally get

$$G = \frac{G_i}{2} = \frac{4e^2}{h} \frac{k_F W}{\pi} \frac{C_2}{2|A_y| l} = \left(\frac{e^2}{h}\right)^2 \frac{4C_2 W n}{|A_y| \sigma(n)}, \tag{10}$$

where C_2 is a numerical coefficient and $\sigma(n)$ is the conductivity of a sample with size $L \gg l$. A formal derivation based on the Green's function formalism yields $C_2 = 4$. For estimate, we can take $n = 10^9$ cm^{-2}, $\sigma \sim 4e^2/h$, $W = 1$ μm, and $A_y = 2 \times 10^5$ cm^{-1}. We then find $G \sim 2e^2/h$, i.e., an appreciably large value.

Scalar potential.—The deformation of the graphene strip also creates a scalar potential $V(x)$ in the system. Our estimates below indicate that it is relatively small.

The bare scalar potential is (assuming $e < 0$):

$$eV_{\text{ext}}(x) = -\frac{P}{n} h(x) + \Theta\left(\frac{L}{2} - |x|\right) \frac{tV_0}{E}, \tag{11}$$

where the first term is the change in electrostatic potential due to the change in distance to the gate, the second term [21,25,26] gives the deformation potential induced by the uniform elongation t/E, and $V_0 \approx 10$ eV.

Within the linear screening theory, the Fourier transform $\tilde{V}$ of V is $\tilde{V}(q) = \tilde{V}_{\text{ext}}(q)/\varepsilon(q)$, where $\varepsilon(q)$ is the dielectric function. For reasonable carrier concentrations we can use the Thomas-Fermi (TF) approximation, $\varepsilon(q) = 1 + k_s/|q|$, where $k_s = 4e^2 k_F/(\epsilon \hbar v)$ is the inverse TF screening length. Potential $V(x)$ can be expressed in terms of special functions. In the limit $k_s L \gg 1$ and at distances greater than k_s^{-1} from the boundaries it reads:

$$eV(x) \simeq \frac{1}{2\pi} \frac{PV_0}{Eh_0 k_s} \frac{L^3}{L^2 - 4x^2} - \frac{8}{\pi} \frac{Ph_0}{nk_s L} \times \left(1 + \frac{x}{L} \ln\left|\frac{L - 2x}{L + 2x}\right|\right). \tag{12}$$

The potential at the edge is given by

$$eV\left(\frac{L}{2} \pm 0\right) = \mp \frac{PV_0 L^2}{16Eh_0} - \frac{4}{\pi} \frac{Ph_0}{nk_s L} [C_3 - \ln(k_s L)], \tag{13}$$

where $C_3 \sim 1$. Thus, the divergences in Eq. (12) are cut off at the distance of the order of the screening length $1/k_s$ from the edge, as expected.

For $n \sim 3 \times 10^{11}$ cm^{-2}, the deformation and the electrostatic potentials at the edges are comparable in magnitude and together amount to about 10% of the Fermi energy. Results for the transmission coefficient including $V(x)$ (whose singularities have been cut off at the distance of 1 nm from the edges) are shown in the right-hand panel of Fig. 4. The scalar potential reduces the Fabry-Pérot oscillations but does not change much in the integrated transmission.

Future directions.—There are a number of possible directions for future study. One interesting problem is how the deformation would affect the quantum Hall effect (QHE) in the suspended graphene. Below we offer a preliminary discussion of this question.

For the model considered, the effects of the deformation are restricted to the $x = \pm L/2$ interfaces. The Landau levels near such lines will be modified (except for the $N = 0$ one, which is topologically protected [27,28]). Quasiclassically, the reflection at the interfaces creates skipping orbits, which propagate parallel to the y axis but in opposite directions on the two sides of each interface. This could lead to backscattering of the edge currents and modification of the QHE. The effect is the strongest when $k_F \lesssim |A_y|$. For low-lying Landau levels, where $k_F \sim 1/l_B$, an estimate of the external magnetic field B_* below which the QHE is affected can be derived from the condition $l_B(B_*) \sim |A_y|^{-1}$. For $\Delta L = -2$ nm, and $A_y \sim 2 \times 10^5$ cm^{-1}, it yields $B_* \sim 0.7$ T.

In a more realistic geometry, a small pseudomagnetic field will also exist inside the suspended region. Its magnitude is of the order of 0.05 T for the same ΔL and L. Landau levels mixing in the bulk occurs when the external field is comparable or smaller than this value.

This work was supported by MEC (Spain) through Grant No. FIS2005-05478-C02-01 and CONSOLIDER CSD2007-00010, by the Comunidad de Madrid, through CITECNOMIK, CM2006-S-0505-ESP-0337, by the EU Contract No. 12881 (NEST), by the Stichting voor Fundamenteel Onderzoek der Materie (FOM) (the Netherlands), and by the US NSF under Grant No. DMR-0706654. We thank B. I. Shklovskii and M. A. H. Vozmediano for discussions.

[1] K. S. Novoselov *et al.*, Science **306**, 666 (2004).
[2] K. S. Novoselov *et al.*, Nature (London) **438**, 197 (2005).
[3] Y. Zhang, Y. W. Tan, H. L. Stormer, and P. Kim, Nature (London) **438**, 201 (2005).
[4] J. C. Meyer *et al.*, Nature (London) **446**, 60 (2007).
[5] J. S. Bunch *et al.*, Science **315**, 490 (2007).
[6] Garcia-Sanchez *et al.*, Nano Lett. **8**, 1399 (2008).
[7] C. Lee, X. Wei, J. W. Kysar, and J. Hone, Science **321**, 385 (2008).
[8] T. J. Booth *et al.*, Nano Lett. **8**, 2442 (2008).
[9] J. S. Bunch *et al.*, Nano Lett. **8**, 2458 (2008).
[10] A. K. Geim and K. S. Novoselov, Nature Mater. **6**, 183 (2007).
[11] M. I. Katsnelson and K. S. Novoselov, Solid State Commun. **143**, 3 (2007).
[12] A. H. Castro Neto, F. Guinea, N. M. R. Peres, K. S. Novoselov, and A. K. Geim, arXiv:0709.1163 [Rev. Mod. Phys. (to be published)].
[13] K. I. Bolotin *et al.*, Solid State Commun. **146**, 351 (2008).
[14] X. Du, I. Skachko, A. Barker, and E. Y. Andrei, Nature Nanotech. **3**, 491 (2008).
[15] G. Li, A. Luican, and E. Y. Andrei, arXiv:0803.4016 (unpublished).
[16] Bolotin *et al.*, Phys. Rev. Lett. **101**, 096802 (2008).
[17] S. P. Timoshenko and S. Woinowsky-Kreiger, *Theory of Plates and Shells* (McGraw-Hill, New York, 1959).
[18] A. Fasolino, J. H. Los, and M. I. Katsnelson, Nature Mater. **6**, 858 (2007).
[19] S. V. Morozov *et al.*, Phys. Rev. Lett. **97**, 016801 (2006).
[20] J. L. Mañes, Phys. Rev. B **76**, 045430 (2007).
[21] H. Suzuura and T. Ando, Phys. Rev. B **65**, 235412 (2002).
[22] F. Guinea, B. Horovitz, and P. Le Doussal, Phys. Rev. B **77**, 205421 (2008).
[23] A. De Martino, L. Dell'Anna, and R. Egger, Phys. Rev. Lett. **98**, 066802 (2007).
[24] C. W. J. Beenakker, Rev. Mod. Phys. **69**, 731 (1997).
[25] S. Ono and K. Sugihara, J. Phys. Soc. Jpn. **21**, 861 (1966).
[26] The total stress tensor includes contributions from the in plane and out of plane displacements, and it is constant within the deformed region [22].
[27] A. J. M. Giesbers *et al.*, Phys. Rev. Lett. **99**, 206803 (2007).
[28] F. Guinea, M. I. Katsnelson, and M. A. H. Vozmediano, Phys. Rev. B **77**, 075422 (2008).